iJRASET
International Journal For Research in Applied Science and Engineering Technology

INTERNATIONAL JOURNAL FOR RESEARCH

IN APPLIED SCIENCE & ENGINEERING TECHNOLOGY

Volume: 10 **Issue:** IX **Month of publication:** September 2022

DOI: https://doi.org/10.22214/ijraset.2022.46775

www.ijraset.com

Call: 08813907089 | E-mail ID: ijraset@gmail.com

International Journal for Research in Applied Science & Engineering Technology (IJRASET)
ISSN: 2321-9653; IC Value: 45.98; SJ Impact Factor: 7.538
Volume 10 Issue IX Sep 2022- Available at www.ijraset.com

Study and Analysis of Different Absorber Geometry of Compound Parabolic Solar Collector and its Effect on Thermal Efficiency for Heating Water for Sanitary Use

Nishant Kumar[1], Dharamveer Singh[2]
[1, 2]*Deptt.of Mech., R. D. Engg College of Engg. Ghaziabad, U.P. 201206*

Abstract: ***This project is focused on carrying out a study of the absorber geometry of the parabolic solar collector compound for heating water for sanitary use, to evaluate the temperature gradient between the inlet and outlet of the water of this concentraDDDtor collector, and the efficiency achieved according to the absorber configuration to later compare it with collectors with a conventional flat absorber surface. The parabola of the reflector of the composite parabolic solar collector was obtained considering the circular absorber, with a concentration ratio of 4 plus 10% of this, to consider a truncation of the reflector, the circular absorber was configured with a small absorber plate of aluminum which has a thermal conductivity of 401 W /mK The values obtained experimentally in the collector were based on the data collected in the field files. It was considered to experience the heating of water on different days with the climatic conditions, cloudy, partially cloudy and sunny, with a totally clear sky. The water heating tests were carried out with two types of geometric configuration of the absorber of the composite parabolic solar collector; circular absorber and configured circular absorber, with which a water outlet temperature of 61 ° C and 76 ° C and a thermal efficiency of 60% respectively were obtained, these results were presented taking into account a climatic condition (sunny day) approximately the same for the two absorber configurations, and with average values of wind speed, ambient temperature and solar radiation.***

Keywords: ***parabolic solar, concentrator collector, flat absorber, concentration ratio, absorber geometry, sanitary, composite parabolic solar collector, ambient temperature, solar radiation***

I. INTRODUCTION

In the world, in recent years there has been a notable increase in solar thermal energy installations; Technological advances allow the manufacture of better quality systems at a lower cost and society is understanding the need to replace fossil fuels.

Since its first invention, several decades ago, various forms of solar thermal collectors have been developed, ranging from flat collectors to parabolic collectors and heliostats. For this reason, the use of solar thermal energy, beyond being an ecological alternative, has become an economically attractive and competitive technology in many countries.

Research has been carried out to promote the development of clean and renewable energy projects such as wind, hydroelectric, biomass and solar energy. an input for the implementation of technologically efficient production processes such as systems for water heating and swimming pool heating, all this through clean energy and under conditions of strategic advantage for our country due to the radiation it receives due to its geographical position

II. PROBLEM DEFINITION

The development of this research is necessary since it seeks to improve the capture of solar energy, studying the geometry of the absorber of the composite parabolic solar collector since it is one of the most used devices, especially due to its great capacity in energy concentration. The surface of the receiver or absorber can have different shapes; the most used form is the configuration with a flat receiver, on the other hand with the cylindrical form the face to the sun can capture direct radiation and the part hides the radiation by reflection. If not carried out, we will not be able to verify if this device will reach significantly higher temperatures, minimize losses, and thus achieve adequate efficiency in heating water for sanitary use.

Will the application of the absorber geometry of the composite parabolic solar collector allow us to achieve significantly higher temperatures for heating water for sanitary use?

With the development of this study, will an acceptable efficiency be determined for heating water for sanitary use using solar radiation?

Will this study know the energy advantage when configuring the absorber of the composite parabolic solar collector?

III. ANALYSIS AND INTERPRETATION OF RESULTS

The water heating tests were carried out using a parabolic solar collector composed of a circular absorber (recommends copper pipe as a material for the circulation of the working fluid).

It was considered to experience the heating of water on different days with the following climatic conditions:

1) Cloudy
2) Partial cloudy
3) Sunny, with a totally clear sky.

A. Water Heating Using The Circular Absorber

The climatic conditions: partially cloudy, sunny and cloudy, respectively.
The outlet temperature of the water from the solar collector was analyzed, which depends on the temperature reached at the focus of concentration of the composite parabolic solar collector, which is the circular absorber.

B. Variation In Temperature Between The Water Inlet And Outlet Of The Solar Collector On A Cloudy Day

The outlet temperature for this climatic condition presented an average of 30.2 ° C, while the average inlet temperature that oscillates 17.2 ° C, having a temperature variation of 13 ° C.

Table 1: Variation of water inlet and outlet temperatures in the composite parabolic solar collector, 19 August 2020.

No.	HOUR	TEMPERATUREWATER INLET TO COLLECTOR Ti (° C)	TEMPERATURECIRCULAR ABSORBER T abs (° C)	TEMPERATUREWATER OUTLET FROM MANIFOLD Ts (° C)	DIFFERENTIAL OUTLET TEMPERATURE - COLLECTOR INLET ΔT (° C)
1	10:00	16.0	22.9	23.0	7.0
2	10:15	16.0	23.6	23.7	7.7
3	10:30	16.0	24.0	24.1	8.1
4	10:45	16.1	26.4	26.5	10.4
5	11:00	16.7	26.4	26.5	9.8
6	11:15	16.8	26.9	27.0	10.2
7	11:30	17.2	28.0	28.1	10.9
8	11:45	18.2	33.0	33.1	14.9
9	12:00	18.2	36.1	36.2	18.0
10	12:15	17.1	34.8	34.9	17.8
11	12:30	16.6	30.0	30.1	13.5
12	12:45	16.9	30.2	30.3	13.4
13	13:00	17.1	32.0	32.1	15.0
14	13:15	17.1	31.5	31.6	14.5
15	13:30	17.1	29.6	29.7	12.6
16	13:45	17.1	28.6	28.7	11.6
17	14:00	17.6	32.4	32.5	14.9
18	14:15	18.3	34.0	34.1	15.8
19	14:30	18.2	32.7	32.8	14.6
20	14:45	17.8	29.5	29.6	11.8
21	15:00	19.7	39.3	39.4	19.7
Average:		17.2	30.1	30.2	13.0

C. Variation In The Temperature Between The Water Inlet And Outlet Of The Collector On A Partly Cloudy Day

For this climatic condition, the outlet temperature presented an average of 43.2 ° C, while the average inlet temperature was around 19.3 ° C, with a temperature variation of 23.8 ° C.

Table 2: Variation of water inlet and outlet temperatures of the composite parabolic solar collector, 29 July 2020.

No.	HOUR	TEMPERATUREWATER INLET TO COLLECTOR Ti (° C)	TEMPERATURE CIRCULAR ABSORBER T abs (° C)	COLLECTOR WATER OUTLET TEMPERATURE Ts (° C)	DIFFERENTIAL OUTLET TEMPERATURE - COLLECTOR INLET ΔT (° C)
1	10:00	16.0	32.9	33.0	17.0
2	10:15	16.1	34.3	34.4	18.3
3	10:30	16.0	34.9	35.0	19.0
4	10:45	16.5	36.1	36.2	19.7
5	11:00	19.9	40.0	40.1	20.2
6	11:15	19.2	41.3	41.4	22.2
7	11:30	18.9	37.6	37.7	18.8
8	11:45	19.5	36.3	36.4	16.9
9	12:00	21.1	37.1	37.2	16.1
10	12:15	22.1	39.1	39.2	17.1
11	12:30	20.3	48.2	48.3	28.0
12	12:45	19.3	49.0	49.1	29.8
13	13:00	20.3	47.8	47.9	27.6
14	13:15	19.0	51.4	51.5	32.5
15	13:30	19.3	45.1	45.2	25.9
16	13:45	19.4	43.8	43.9	24.5
17	14:00	21.5	51.6	51.7	30.2
18	14:15	20.1	51.8	51.9	31.8
19	14:30	20.4	49.6	49.7	29.3
20	14:45	20.5	49.2	49.3	28.8
21	15:00	20.8	47.1	47.2	26.4
Average:		19.3	43.1	43.2	23.8

D. Temperature Variation Between The Water Inlet And Outlet Of The Solar Collector On A Sunny Day

The outlet temperature for this climatic condition presented an average of 61.7 ° C, while the average inlet temperature was around 22.3 ° C, with a temperature variation of 39.4 ° C.

Table 3: Variation of water inlet and outlet temperatures of the composite parabolic solar collector, 12 June 2020

No.	HOUR	TEMPERATUREWATER INLET TO COLLECTOR Ti (° C)	TEMPERATURECIR CULAR ABSORBER T abs (° C)	COLLECTOR WATER OUTLET TEMPERATURE Ts (° C)	DIFFERENTIAL OUTLET TEMPERATURE - COLLECTOR INLET ΔT (° C)
1	10:00	15.8	38.5	38.6	22.8
2	10:15	16.9	45.8	45.9	29.0
3	10:30	23.5	48.3	48.4	24.9
4	10:45	27.8	57.9	58.0	30.2
5	11:00	31.3	60.7	60.8	29.5
6	11:15	33.8	65.6	65.7	31.9
7	11:30	35.1	70.4	70.5	35.4
8	11:45	20.5	67.7	67.8	47.3
9	12:00	19.1	68.2	68.3	49.2
10	12:15	19.6	65.7	65.8	46.2
11	12:30	19.9	66.1	66.2	46.3
12	12:45	20.3	62.3	62.4	42.1
13	13:00	19.8	67.0	67.1	47.3
14	13:15	19.9	66.9	67.0	47.1
15	13:30	20.2	63.6	63.7	43.5
16	13:45	20.2	64.4	64.5	44.3
17	14:00	20.8	64.6	64.7	43.9
18	14:15	20.3	62.6	62.7	42.4
19	14:30	21.9	63.1	63.2	41.3
20	14:45	21.3	63.0	63.1	41.8
21	15:00	21.3	61.5	61.6	40.3
Average:		22.3	61.6	61.7	39.4

E. Thermal Efficiency Of The Compound Parabolic Solar Collector

For each efficiency data in the test interval, the efficiency value was calculated using equation proposed by ANSI / ASHRAE 93-1986:

$$\eta_g = \frac{\int_{t1}^{t2} \dot{m}\, C_p\, (T_s - T_i)\, dt}{A_g \int_{t1}^{t2} G_T\, dt}$$

*You*Water temperature at collector inlet (° C) Ts Water temperature at collector outlet (° C) Ag Gross area of solar collector (m2)
*Gb*Direct radiation incident on the collector (W / m2)
t1 and t2 Time start and end of the test interval (minutes) dt derived from the variable with respect to time t

Equation (4.1) can be expressed as follows:

$$\eta_g = \frac{\dot{m}\, C_p \int_{t1}^{t2} (T_s - T_i)\, dt}{A_g \int_{t1}^{t2} G_T\, dt}$$

Ag = length * width = 1.535m * 0.85m = 1.305 m2

$\dot{m}$ = 0.003 kg / s through equation (2.35) with water density values of ρwater = 997 kg / m3 average water velocity vprom = 0.01 m / s assumed according to Toalombo (2011) which specifies that the flow velocity of liquids inside pipes does not exceed 3m / s; and a cross-sectional area of the duct (circular absorber) Ac = 0.00028 m2. The two integrals of equation were developed separately and assuming the values of $\dot{m}$, Cp and Ag as constants. To solve the integrals of equation the Toalombo trapezoid method (2011) was applied, which assumes a linear behavior of both (ΔT = Ts - Ti) and of the direct radiation Gb incident on the solar collector in fifteen minute intervals.

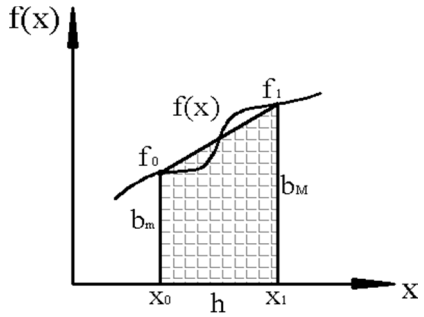

Figure 1: Definition of the Trapezoid Method to determine the area under a curve.

$$A = \frac{h\,(b_m + b_M)}{2}$$

$$A = \int_{x0}^{x1} f(x)\,dx \approx \frac{(x_1 - x_0)(f_0 + f_1)}{2}$$

According to the data of direct radiation Gb incident on the solar collector, obtained from Annex A, for each day analyzed, the stored energy was obtained in fifteen-minute intervals applying the trapezoid method to solve equation

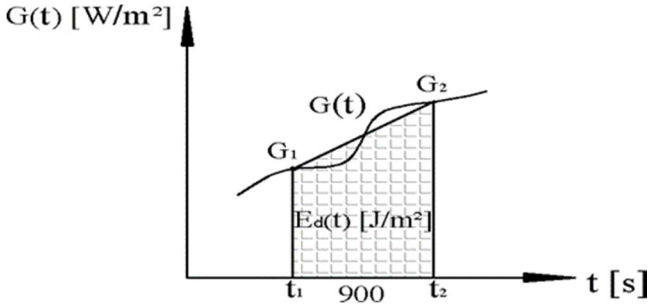

Figure 2: Definition of the trapezoid method to determine the energy stored in the solar collector in fifteen minute intervals.

$$Ea = \int_{t1}^{t2} G_b\, dt \approx \frac{(t_2 - t_1)(G_{b_1} + G_{b_2})}{2} \approx \sum_{i=1}^{N-1} 450\,(G_{b_i} + G_{b_{i+1}})$$

According to Toalombo (2011), it is possible to determine the variation in temperatures between the outlet and inlet of the panel with respect to time in fifteen-minute intervals using the trapezoid method to solve equation and add the partials.

$$\int_{t1}^{t2} \Delta T\, dt = \int_{t1}^{t2} (T_s - T_i)\, d_t \cong \sum_{i=1}^{N-1} 450\,(\Delta T_i + \Delta T_{i+1})$$

F. Thermal Efficiency On A Cloudy Day

Through equation, the energy was calculated in 15-minute intervals and the partials were added for the total by applying the trapezoid method for approximation of areas and whose values are presented in table 4

Table 4: Energy stored in the collector (19-August-2020)

HOUR (hh: mm)	RADIATION DIRECT INCIDENT IN THE COLLECTOR Gb (W / m²)	ENERGY EVERY 15MIN Ea (J / m²)	ACCUMULATED ENERGY Ea (J / m²)
10:00	147.04	0	0
10:15	172.36	143730	143730
10:30	150.19	145144	288875
10:45	188.33	152331	441206
11:00	198.52	174082	615288
11:15	204.40	181317	796604
11:30	248.23	203688	1000292
11:45	265.50	231180	1231472
12:00	245.10	229770	1461243
12:15	202.94	201617	1662860
12:30	183.69	173982	1836842
12:45	191.68	168919	2005 761
13:00	201.75	177046	2182807
13:15	191.39	176914	2359722
13:30	194.31	173567	2533289
13:45	212.17	182916	2716205
14:00	195.19	183309	2899513
14:15	175.66	166882	3066395
14:30	309.70	218412	3284807
14:45	366.90	304471	3589279
15:00	205.94	257779	3847058

By means of equation, the temperature variation in 15-minute intervals was determined, the results of which are presented in Table 5.

Table 5: Integration of the variation in temperature between the inlet and outlet of the collector water as a function of time (19-August-2020)

HOUR (hh: mm)	WEATHER t (s)	Ti (° C)	Ts (° C)	ΔT (° C)	$\int_{t1}^{t2} (T_s - T_i) dt$ (s ° C)
10:00	0	16.0	23.0	7.0	0
10:15	900	16.0	26.4	10.4	7830
10:30	1800	16.0	24.1	8.1	16155
10:45	2700	16.1	26.5	10.4	24480
11:00	3600	16.7	26.5	9.8	33570
11:15	4500	16.8	27.0	10.2	42570
11:30	5400	17.2	28.1	10.9	52065
11:45	6300	18.2	33.1	14.9	63675
12:00	7200	18.2	36.2	18.0	78480
12:15	8100	17.1	34.9	17.8	94590
12:30	9000	16.6	30.1	13.5	108675
12:45	9900	16.9	30.3	13.4	120780
13:00	10800	17.1	32.1	15.0	133560
13:15	11700	17.1	31.6	14.5	146835
13:30	12600	17.1	29.7	12.6	159030
13:45	13500	17.1	28.7	11.6	169920
14:00	14400	17.6	32.5	14.9	181845
14:15	15300	18.3	34.1	15.8	195660
14:30	16200	18.2	32.8	14.6	209340
14:45	17100	17.8	29.6	11.8	221220
15:00	18000	19.7	39.4	19.7	235395

Table 6 shows the thermal efficiency values determined by equation in 15-minute intervals with the values obtained in Tables 4 and 5.

Table 6: Thermal efficiency of the composite parabolic solar collector (19 August 2020).

HOUR (hh: mm)	g (%)
10:00	-
10:15	52.3480
10:30	53.7384
10:45	53.3159
11:00	52.4276
11:15	51.3509
11:30	50.0157
11:45	49.6857
12:00	51,6088
12:15	54.6609
12:30	56.8519
12:45	57.8633
13:00	58.7960
13:15	59.7938

13:30	60.3228
13:45	60.1131
14:00	60.2647
14:15	61.3142
14:30	61.2392
14:45	59.2249
15:00	58.7971

G. Thermal Efficiency On A Partly Cloudy Day

Through equation the energy was calculated in 15-minute intervals and the partials were added for the total by applying the trapezoid method for approximation of areas and whose values are presented in table 7 for a partial cloudy day.

Table 7: Energy stored in the collector (29 July 2020)

HOUR (hh: mm)	DIRECT INCIDENT RADIATION IN THE COLLECTOR Gb (W / m²)	ENERGY EVERY 15MIN Ea (J / m²)	ACCUMULATED ENERGY Ea (J / m²)
10:00	186,134	0	0
10:15	211,865	179100	179100
10:30	244,578	205400	384499
10:45	394,813	287726	672225
11:00	408,378	361436	1033661
11:15	397,212	362515	1396176
11:30	265,660	298293	1694469
11:45	282,711	246767	1941236
12:00	250,426	239912	2181148
12:15	366,084	277430	2458578
12:30	383,962	337521	2796099
12:45	270,439	294480	3090579
13:00	416,127	308955	3399534
13:15	271,648	309499	3709033
13:30	332,840	272020	3981053
13:45	380,382	320950	4302003
14:00	328,499	318997	4621000
14:15	327,547	295221	4916221
14:30	213,622	243526	5159747
14:45	177,850	176162	5335909
15:00	123,333	135532	5471441

By means of equation, the temperature variation for a cloudy partial day was determined, in 15-minute intervals, the results of which are presented in Table 8.

Table 8: Integration of the variation in temperature between the inlet and outlet of the collector water as a function of time (29 July 2020)

HOUR (hh: mm)	WEATHER t (s)	Ti (° C)	Ts (° C)	ΔT (° C)	$\int_{t1}^{t2} (T_s - T_i) dt$ (s ° C)
10:00	0	16.0	33.0	17.0	0
10:15	900	16.1	34.4	18.3	15885
10:30	1800	16.0	35.0	19.0	32670
10:45	2700	16.5	36.2	19.7	50085
11:00	3600	19.9	40.1	20.2	68040
11:15	4500	19.2	41.4	22.2	87120
11:30	5400	18.9	37.7	18.8	105570
11:45	6300	19.5	36.4	16.9	121635
12:00	7200	21.1	37.2	16.1	136485
12:15	8100	22.1	39.2	17.1	151425
12:30	9000	20.3	48.3	28.0	171720
12:45	9900	19.3	49.1	29.8	197730
13:00	10800	20.3	47.9	27.6	223560
13:15	11700	19.0	51.5	32.5	250605
13:30	12600	19.3	45.2	25.9	276885
13:45	13500	19.4	43.9	24.5	299565
14:00	14400	21.5	51.7	30.2	324180
14:15	15300	20.1	51.9	31.8	352080
14:30	16200	20.4	49.7	29.3	379575
14:45	17100	20.5	49.3	28.8	405720
15:00	18000	20.8	47.2	26.4	430560

Table 9 shows the thermal efficiency values determined by equation in 15-minute intervals with the values obtained in Tables 7 and 8 for a partially cloudy day.

Table 9: Thermal efficiency of the composite parabolic solar collector (29 July 2020).

HOUR (hh: mm)	g (%)
10:00	-
10:15	85.23
10:30	81.65
10:45	71.59
11:00	63.25
11:15	59.96
11:30	59.87
11:45	60.21
12:00	60.13
12:15	59.18
12:30	59.01
12:45	61.48
13:00	63.19
13:15	64.93
13:30	66.83
13:45	66.91
14:00	67.41
14:15	68.82
14:30	70.69
14:45	73.06
15:00	75.62

H. Thermal Efficiency On A Sunny Day

Through equation the energy was calculated in 15-minute intervals and the partials were added for the total by applying the trapezoid method for approximation of areas and whose values are presented in table 10 for a sunny day.

Table 4.10: Energy stored in the collector (12 June 2020)

HOUR (hh: mm)	DIRECT INCIDENT RADIATION IN THE COLLECTOR Gb (W / m²)	ENERGY EVERY 15MIN Ea (J / m²)	ACCUMULATED ENERGY Ea (J / m²)
10:00	393,550	0	0
10:15	441,202	375638	375638
10:30	469,822	409960	785599
10:45	545,177	456749	1242348
11:00	556,543	495774	1738122
11:15	615,222	527294	2265416
11:30	695,368	589766	2855182
11:45	642,843	602195	3457377
12:00	683,268	596750	4054127
12:15	664,900	606675	4660803
12:30	655,145	594020	5254823
12:45	634,527	580352	5835175
13:00	622,519	565671	6400846
13:15	600,284	550261	6951107
13:30	581,921	531992	7483099
13:45	553,511	510944	7994044
14:00	519,164	482704	8476748
14:15	550,152	481192	8957940
14:30	459,349	454275	9412216
14:45	435,954	402887	9815102
15:00	322,393	341256	10156358

By means of equation, the temperature variation for a sunny day was determined, in 15-minute intervals, the results of which are presented in Table 11.

Table 4.11: Integration of the temperature variation between the water inlet and outlet of the collector as a function of time (12 June 2020)

HOUR (hh: mm)	WEATHER t (s)	Ti (° C)	Ts (° C)	ΔT (° C)	$\int_{t1}^{t2}(T_s - T_i)dt$ (s ° C)
10:00	0	15.8	38.6	22.8	0
10:15	900	16.9	45.9	29.0	23310
10:30	1800	23.5	48.4	24.9	47565
10:45	2700	27.8	58.0	30.2	72360
11:00	3600	31.3	60.8	29.5	99225
11:15	4500	33.8	65.7	31.9	126855
11:30	5400	35.1	70.5	35.4	157140
11:45	6300	20.5	67.8	47.3	194355
12:00	7200	19.1	68.3	49.2	237780
12:15	8100	19.6	65.8	46.2	280710
12:30	9000	19.9	66.2	46.3	322335
12:45	9900	20.3	62.4	42.1	362115
13:00	10800	19.8	67.1	47.3	402345
13:15	11700	19.9	67.0	47.1	444825
13:30	12600	20.2	63.7	43.5	485595
13:45	13500	20.2	64.5	44.3	525105
14:00	14400	20.8	64.7	43.9	564795
14:15	15300	20.3	62.7	42.4	603630
14:30	16200	21.9	63.2	41.3	641295
14:45	17100	21.3	63.1	41.8	678690
15:00	18000	21.3	61.6	40.3	715635

Table 12 shows the thermal efficiency values determined by equation in 15-minute intervals with the values obtained in Tables 10 and 11 for a sunny day.

Table 4.12: Thermal efficiency of the composite parabolic solar collector (12 June 2020).

HOUR (hh: mm)	ηg (%)
10:00	-
10:15	59.63
10:30	58.18
10:45	55.97
11:00	54.86
11:15	53.81
11:30	52.89
11:45	54.02
12:00	56.36
12:15	57.87
12:30	58.94
12:45	59.63
13:00	60.40
13:15	61.49
13:30	62.36
13:45	63.12
14:00	64.02
14:15	64.75
14:30	65.47
14:45	66.45
15:00	67.71

I. Data Interpretation

From the values established in literal (4.1), the scatter graphs were made in which the outlet temperature, solar radiation as a function of time was analyzed, and the efficiency curve was obtained from the efficiency ratio collector thermal as a function of the ratio of the water inlet temperature to the collector Ti minus the ambient temperature Ta on the direct component of the incident radiation on the solar collector; according to the geometric configuration of the absorber of the composite parabolic solar collector.

Graph 1: Outlet temperature vs Weather, 19 August 2020 cloudy (circular absorber).

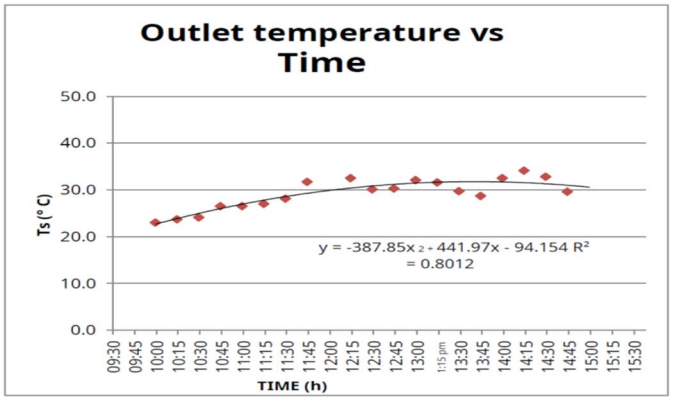

Graph 1 shows the temperature variation for 19 August 2020, with a cloudy weather condition, which tends to a quadratic distribution curve. The outlet temperature has an unstable behavior and presents a value of 34.8 ° C as its highest peak. minus the ambient temperature on the direct component of the incident radiation in the solar collector, for 19 August 2020.

Table 13: Inlet temperature difference minus outlet temperature relation on the direct component of the incident radiation in the collector, 19 August 2020.

No.	HOUR	TEMPERATUREAMBIENT Ta (° C)	TEMPERATUREWATER INLET TO COLLECTOR Ti (° C)	DIRECT INCIDENT RADIATION IN THE COLLECTOR Gb (W / m²)	(Ti-Ta) / Gb
1	10:00	16.1	16.0	147.04	-0.001
2	10:15	16.5	16.0	172.36	-0.003
3	10:30	16.4	16.0	150.19	-0.003
4	10:45	16.7	16.1	188.33	-0.003
5	11:00	16.5	16.7	198.52	0.001
6	11:15	16.8	16.8	204.40	0.000
7	11:30	15.9	17.2	248.23	0.005
8	11:45	21.8	18.2	265.50	-0.014
9	12:00	17.1	18.2	245.10	0.004
10	12:15	16.9	17.1	202.94	0.001
11	12:30	17.8	16.6	183.69	-0.007
12	12:45	16.8	16.9	191.68	0.001
13	13:00	17.5	17.1	201.75	-0.002
14	13:15	16.9	17.1	191.39	0.001
15	13:30	17.8	17.1	194.31	-0.004
16	13:45	17.6	17.1	212.17	-0.002
17	14:00	18.3	17.6	195.19	-0.004
18	14:15	19.6	18.3	175.66	-0.007
19	14:30	19.8	18.2	309.70	-0.005
20	14:45	17.2	17.8	366.90	0.002
21	15:00	19.3	19.7	205.94	0.002

Efficiency of the table 6 and the values of the relation of the inlet temperature minus the ambient temperature on the direct component of the incident radiation in the solar collector of the table 13.

Graph 2: Thermal Efficiency, 19 August 2020- cloudy (circular absorber).

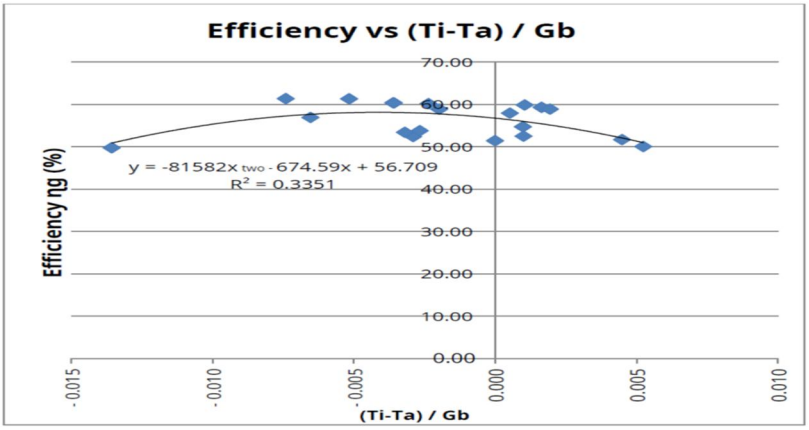

For this climatic condition the graph produces a quadratic distribution curve, between the thermal efficiency of the solar collector and the relation of the inlet temperature minus the ambient temperature on the direct component of the incident radiation in the collector, which shows us for a cloudy day, thermal efficiency values between 50% and 61%.

Graph 3: Outlet temperature vs Time, 29 July 2020- partial cloudy (circular absorber).

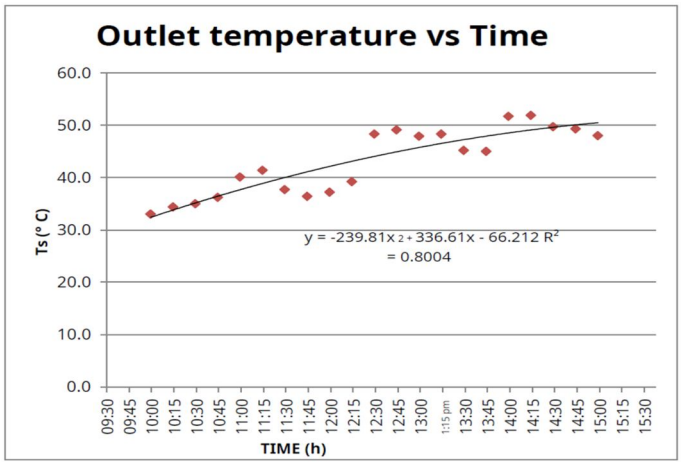

Graph 3 shows the variation of the outlet temperature for 29 July 2020, with a partially cloudy climatic condition, which tends towards an increasing quadratic distribution curve, having a maximum value of 51.9 ° C. and a minimum value of 33 ° C for the collector outlet water temperature minus the ambient temperature on the direct component of the incident radiation in the solar collector, for 29 July 2020.

Table 14: Inlet temperature difference minus outlet temperature relation on the direct component of the incident radiation in the collector, 29 July 2020.

No.	HOUR	TEMPERATUREAMBIENT Ta (° C)	TEMPERATUREWATER INLET TO COLLECTOR Ti (° C)	DIRECT INCIDENT RADIATION IN THE COLLECTOR Gb (W / m²)	(Ti-Ta) / Gb
1	10:00	20.8	16.0	186.13	-0.03
2	10:15	22.4	16.1	211.87	-0.03
3	10:30	23.4	16.0	244.58	-0.03
4	10:45	22.9	16.5	394.81	-0.02
5	11:00	27.3	19.9	408.38	-0.02
6	11:15	28.0	19.2	397.21	-0.02
7	11:30	22.8	18.9	265.66	-0.01
8	11:45	23.2	19.5	282.71	-0.01
9	12:00	23.8	21.1	250.43	-0.01
10	12:15	23.1	22.1	366.08	0.00
11	12:30	19.8	20.3	383.96	0.00
12	12:45	22.9	19.3	270.44	-0.01
13	13:00	21.6	20.3	416.13	0.00
14	13:15	21.3	19.0	271.65	-0.01
15	13:30	22.8	19.3	332.84	-0.01
16	13:45	23.1	19.4	380.38	-0.01
17	14:00	24.8	21.5	328.50	-0.01
18	14:15	23.9	20.1	327.55	-0.01
19	14:30	23.5	20.4	213.62	-0.01
20	14:45	21.9	20.5	177.85	-0.01
21	15:00	19.8	20.8	123.33	0.01

Efficiency of the table 7 and the values of the relation of the inlet temperature minus the ambient temperature on the direct component of the incident radiation in the solar collector of the table 14.

Graph 4: Thermal Efficiency, 29 July 2020 - partly cloudy (circular absorber).

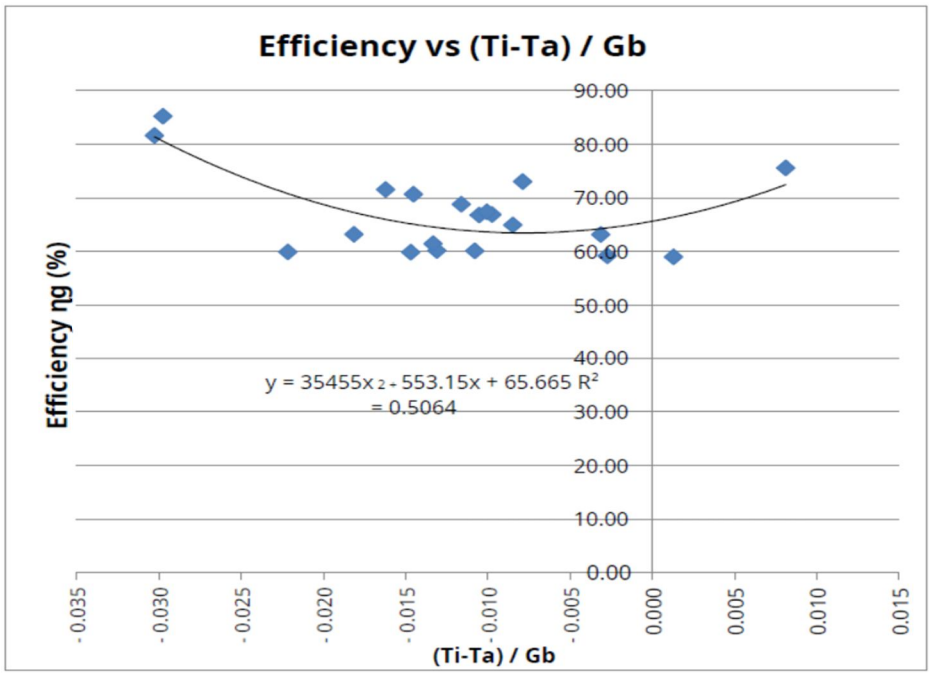

For this climatic condition, the graph produces a quadratic distribution between the thermal efficiency of the system and the relation of the inlet temperature minus the ambient temperature on the direct component of the incident radiation in the solar collector, which shows us for a partially cloudy day, thermal efficiency values between 59% and 85%.

Graph 5: Outlet temperature vs Time, 12 June 2020 - sunny (circular absorber).

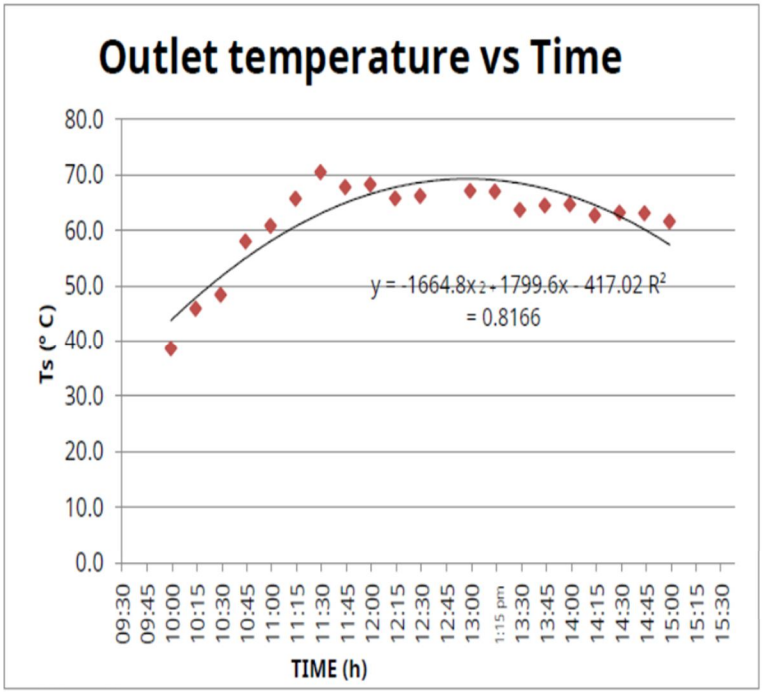

Graph 5 shows the variation in temperature for 12 June 2020, with a sunny weather condition, which tends to a quadratic distribution curve. The highest peak has a value of 70.4 ° C, and has stable values between 60 and 65 ° C as of 11:00 minus the ambient temperature on the direct component of the incident radiation in the solar collector, for 12 June 2020.

Table 15: Inlet temperature difference minus outlet temperature ratio on the direct component of incident radiation in the collector, 12 June 2020.

No.	HOUR	TEMPERATUREAMBIENT Ta (° C)	TEMPERATUREWATER INLET TO COLLECTOR Ti (° C)	DIRECT INCIDENT RADIATION IN THE COLLECTOR Gb (W / m²)	(Ti-Ta) / Gb
1	10:00	27.2	15.8	393.55	-0.03
2	10:15	27.9	16.9	441.20	-0.02
3	10:30	27.4	23.5	469.82	-0.01
4	10:45	22.1	27.8	545.18	0.01
5	11:00	24.1	31.3	556.54	0.01
6	11:15	26.2	33.8	615.22	0.01
7	11:30	28.5	35.1	695.37	0.01
8	11:45	27.8	20.5	642.84	-0.01
9	12:00	25.1	19.1	683.27	-0.01
10	12:15	23.5	19.6	664.90	-0.01
11	12:30	23.3	19.9	655.14	-0.01
12	12:45	22.7	20.3	634.53	0.00
13	13:00	22.3	19.8	622.52	0.00
14	13:15	26.3	19.9	600.28	-0.01
15	13:30	27.8	20.2	581.92	-0.01
16	13:45	22.1	20.2	553.51	0.00
17	14:00	23.7	20.8	519.16	-0.01
18	14:15	20.6	20.3	550.15	0.00
19	14:30	26.7	21.9	459.35	-0.01
20	14:45	25.9	21.3	435.95	-0.01
21	15:00	24.8	21.3	322.39	-0.01

Efficiency of the table 8 and the values of the relation of the inlet temperature minus the ambient temperature on the direct component of the incident radiation in the solar collector of the table 15.

Graph 6: Thermal Efficiency, 12 June 2020 - sunny (circular absorber).

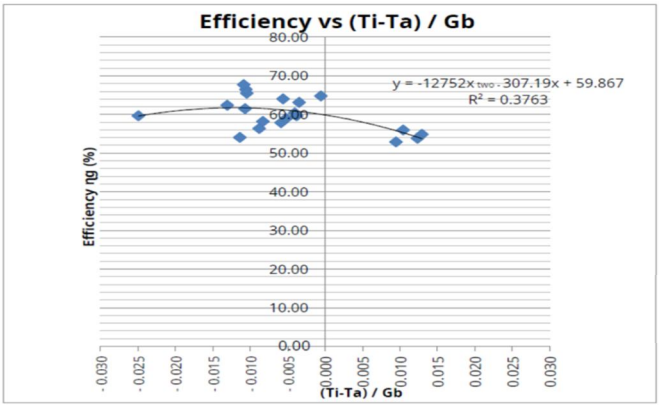

For this climatic condition, the graph produces a quadratic distribution between the thermal efficiency of the collector and the relationship of the inlet temperature minus the ambient temperature on the direct component of the incident radiation in the collector, which shows us, for a sunny day, values of thermal efficiency between 59% and 68%

J. Verification Of The Hypothesis Hypothesis

The use of the circular absorber of the composite parabolic solar collector will allow to achieve higher thermal efficiency than with the conventional flat absorber surface.

Verification

Through the study of the absorber geometry of the composite parabolic solar collector, the thermal efficiency could be determined. To examine the energy stored in the solar collector, equation is expressed as follows:

$$\eta_g = \frac{\dot{m}\, C_p \int_{t1}^{t2} (T_s - T_i)dt}{A_g \int_{t1}^{t2} G_T\, dt}$$

Constant data:

$\dot{m}$ = 0.003 Kg / s Cp = 4180 J / kg ° C Ag = 1.305 m2

The analysis was carried out for three days in different climatic conditions, as shown in Table 16.

Table 4.16: Hypothesis verification (circular absorber).

DAY	CLIMATE CONDITION	ACCUMULATED ENERGY Ea (KJ / m2)	USEFUL HEAT *how useful*(KJ)	INCIDENT HEAT *what incident*(KJ)	THERMAL EFFICIENCY g[%]
08-19-2020	Cloudy	3,847,058	2951.8533	5020.41038	58.80
07-29-2020	Partly Cloudy	5471,441	5399.2224	7140.23044	75.62
06-12-2020	Sunny	10 156,358	8974.0629	13254.04765	67.71

In a conventional flat absorber surface solar heater built at the FICM-UTA, a thermal efficiency of 55.2% was achieved on a sunny day, Toalombo Byron (2011) taking into account the gross area of the collector.

Figure 7 shows the difference in thermal efficiency of a conventional flat absorber surface solar collector and a composite parabolic solar collector with a circular absorber.

Graph 7: Verification of the Hypothesis (circular absorber).

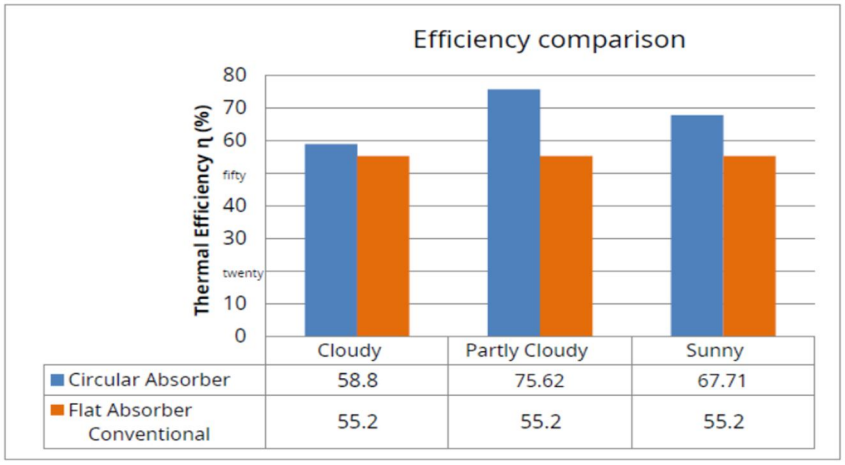

The graph shows that on a sunny day the solar collector with circular absorber exceeds by 12.51% the value of 55.2% of thermal efficiency of the conventional flat absorber surface solar collector; while on a cloudy and cloudy partial day it exceeds this value by 20.42% and 3.6% respectively; with which it can be verified that with the circular absorber of the composite parabolic solar collector it will allow us to achieve greater thermal efficiency than with the conventional flat absorber surface

The configuration of the composite parabolic solar collector concentrates radiation through the use of multiple reflections as well as direct interception, in order to have a greater benefit from solar energy which is naturally available and thus be able to guarantee greater thermal efficiency in solar systems.

IV. CONCLUSIONS

The variation in water temperature between the inlet and outlet of the collector was unstable in the test periods, since as this type of collector is a radiation concentrator, it produces instantaneous temperature increases. The water outlet temperatures of the composite parabolic solar collector with the circular absorber exceeded 60 ° C on a sunny day, with a totally clear sky.

On days with little presence of sun, partially cloudy, the outlet temperature of the water from the solar collector was around 50 ° C, and on a cloudy day it reached temperatures higher than 30 ° C.

On days with partially cloudy and sunny weather conditions, the water outlet temperature was within the indicative range of the composite parabolic solar collector, which is 60 ° C to 240 ° C.

The thermal efficiency achieved in the composite parabolic solar collector with the circular absorber reached a value of 67.71% higher by 12.51% than the value of 55.2% of thermal efficiency of the conventional flat surface solar collector for a sunny day. The thermal efficiency in the parabolic solar collector composed with the circular absorber for days, partially cloudy and cloudy were 75.62% and 58.8% respectively, which exceeded the thermal efficiency value of the conventional flat absorber surface solar collector by 20.42% and 3.6%.

REFERENCES

[1] ANSI / ASHRAE 93-1986. Methods of testing to determine the thermal performance of solar collectors. ASHRAE Standard.
[2] Aguayo, D., Velasquez, N., & Ojeda, S. (2009). Development of a solar heating system and coupling to an anaerobic digester. Retrieved on October 11, 2013, from Redisa:http://www.redisa.uji.es
[3] Byron, T. (2011). Study of the solar irradiation spectrum to determine the potential of usable energy in the city of Ambato. "Mechanical Engineering Thesis". UTA, Ambato, Ecuador.
[4] Campuzano, G. and Chiriboga, J. (2010). Design and construction of an adsorption torque cooling system. "Mechanical Engineering Thesis". EPN, Quito, Ecuador.
[5] Carta, J., Calero, R., Colmenar, A., & Castro, M. (2009). Renewable energy plants. Madrid: Pearson Education.
[6] Cengel,Y. (2007). Heat and mass transfer (Fourth ed.). Mexico: Mc.Graw-Hill.
[7] Duffie,J., & Beckman, W. (1980). Solar engineering of thermal processes.Wisconsin-Madison: Jhon Wiley & Sons, INC.
[8] Echeverría,C. (2011). Design of a composite parabolic trough collector.Retrieved on October 8, 2013, fromhttp://pirhua.udep.edu.pe
[9] Estrada, C., Arancibia, C., Dorantes, R., Islas, J., &Mulhia, I. (2005). Long-term vision on the use of renewable energies in Mexico. Retrieved on November 20, 2013, fromhttp://www.sener.gob.mx
[10] Fernandez, F., Ramos, F., Tinaut, D., Rodriguez, M., Díaz, C., Macias, M., and others. (1987). Methodology and calculation of radiation for concentrating collectors. Madrid: Artegraf.
[11] Gutierrez, J. (2010). Design and characterization of a compound parabolic concentrator. Retrieved on September 10, 2013, fromhttp://www.perusolar.org
[12] InstituteEcuadorian Standardization Inen 2 507: 2009. Thermal performance of solar collectors in water heating systems for sanitary use. Requirements. Quito, Ecuador: INEN.
[13] Jaramillo, A. (2012). Solar concentration and heat from industrial processes_22_FEB_2012. Retrieved on December 5, 2014, fromhttp://www.cie.unam.mx

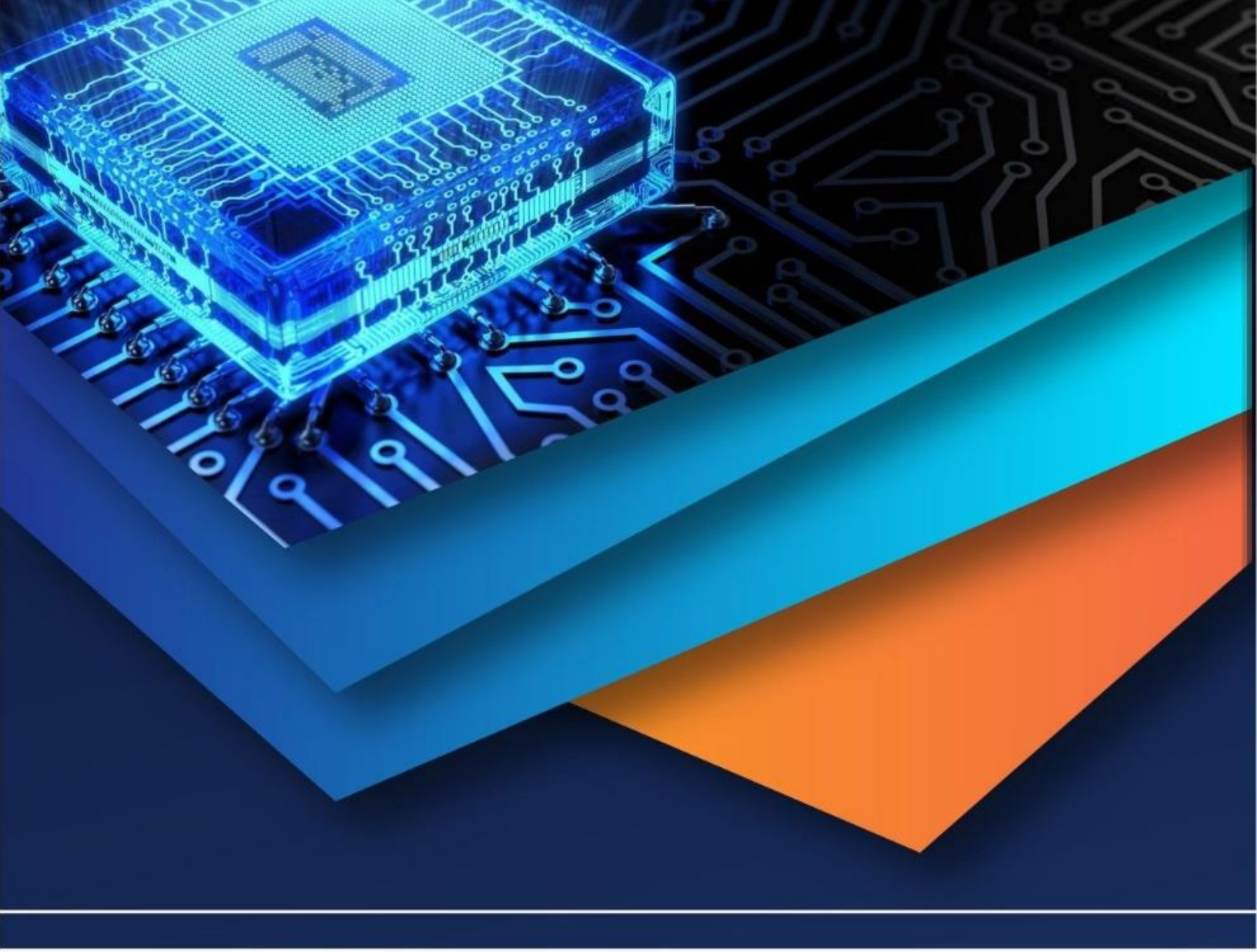

10.22214/IJRASET

45.98

IMPACT FACTOR: 7.129

IMPACT FACTOR: 7.429

INTERNATIONAL JOURNAL FOR RESEARCH

IN APPLIED SCIENCE & ENGINEERING TECHNOLOGY